

IC/97/75  
May 10, 2018

# The $\beta$ -spectrum in presence of background potentials for neutrinos

Francesco Vissani

*International Centre for Theoretical Physics,  
Strada Costiera 11, I-34013 Trieste, Italy*

---

## **Abstract**

We compute the spectrum of  $\beta$ -decay, assuming that (Majorana or Dirac) neutrinos propagate in constant potentials. We study the modifications of the spectrum due to the effect of these potentials. Data on tritium decay and on  ${}^3\text{H}$ - ${}^3\text{He}$  mass difference allow us to infer bounds in the electronvolts range on the potentials.

---

arXiv:hep-ph/9707343v2 19 Jul 1997

We study the modifications of the electron spectrum in  $\beta$ -decay due to hypothetical potentials influencing the electron neutrino propagation. The weak interactions of the neutrinos with ordinary matter do modify the neutrino propagation [1], but are not expected to be able to affect the measured  $\beta$ -spectrum\*. In the present work we take a purely phenomenological point of view, namely we do not attempt a study of the nature of the potentials, but just wonder which kind of observable effects they could produce. Apart from the interest in contemplating a theoretical possibility, some additional motivation for this work comes from anomalies suggested by experimental studies of tritium decay [3, 4].

We show that potentials in the electronvolt range can lead to observable features in the  $\beta$ -spectrum, discuss the features of the spectrum near and far from the endpoint, and use the experimental data to put an upper bound on these potentials.

The structure of the paper is the following: in the first section we review the formalism for treating Majorana or Dirac neutrinos (essentially equivalent to the formalism put forward in [5] for Dirac neutrinos); in the second section we compute the  $\beta$ -spectrum in the presence of a background potential for the neutrino; in the last section we discuss the features of the spectrum, and compare our results with the experimental findings and with other theoretical models.

## 1 Neutrino fields in presence of background potentials

Consider a neutrino described by the bi-spinor  $N_A$  ( $A = 1, 2$ ), that participates in weak interactions and propagates in a constant potential  $V_L$  :

$$\mathcal{L}_M^0 = i\bar{N}\bar{\sigma}_a\partial^aN - (mNN + \text{h.c.}) - V_L\bar{N}N; \quad (1)$$

where  $a = 0, 1, 2, 3$  are Lorentz indices and  $m$  is a Majorana mass. The spinorial contractions<sup>†</sup> imply that all terms but the last one are Lorentz invariants; therefore this latter term implies the existence of a preferential Lorentz frame. Alternatively, assuming that a second bispinor  $N_A^c$  exists, we can consider the propagation described by the lagrangian:

$$\mathcal{L}_D^0 = i\bar{N}\bar{\sigma}_a\partial^aN + i\overline{N^c}\bar{\sigma}_a\partial^aN^c - (mN^cN + \text{h.c.}) - V_L\bar{N}N - V_R\overline{N^c}N^c, \quad (2)$$

where  $m$  now denotes a Dirac mass term.  $N^c$  will be assumed not to participate in the weak interactions. Eq. (2) is invariant under those U(1) transformations that act

---

\*A density of scatterers  $\rho$  of the order of the Avogadro number gives origin to a potential  $V_{weak} \sim G_F\rho \sim 5 \cdot 10^{-14}$  eV, 14 order of magnitudes smaller than the present experimental sensitivity; compare however with [2].

<sup>†</sup>Our conventions for bispinors:  $\overline{N_A} = N_{\dot{A}}$ ;  $N^A = \epsilon^{AB}N_B$  ( $\epsilon$  is asymmetric, and  $\epsilon^{12} = 1$ );  $NN = N^AN_A$ ;  $\bar{\sigma}_a = (\mathbb{1}, \vec{\sigma})$  ( $\vec{\sigma}$  are the Pauli matrices);  $\bar{N}\bar{\sigma}_aN = \bar{N}_{\dot{A}}\bar{\sigma}_a^{\dot{A}B}N_B$ ;  $\bar{N}N = \bar{N}_{\dot{A}}N_A$ .

with opposite charges on  $N$  and  $N^c$  (Majorana mass terms like  $NN$  and/or potential terms like  $\overline{N^c}N$  explicitly break this invariance). Introducing the four-spinors:

$$\nu_\alpha^M = \begin{pmatrix} N_A \\ \overline{N^A} \end{pmatrix} \quad [\text{Majorana}] \quad \text{and} \quad \nu_\alpha^D = \begin{pmatrix} N_A \\ \overline{N^c A} \end{pmatrix} \quad [\text{Dirac}], \quad (3)$$

we can rewrite the lagrangians (1) and (2), after performing a partial integration in the corresponding actions, in the following form:

$$\begin{aligned} \mathcal{L}_M^0 &= \frac{1}{2} \overline{\nu^M} [i\gamma_a \partial^a - m + \gamma^0 \gamma^5 V_L] \nu^M \quad \text{and} \\ \mathcal{L}_D^0 &= \overline{\nu^D} [i\gamma_a \partial^a - m - \gamma^0 (V_S - \gamma^5 V_D)] \nu^D. \end{aligned} \quad (4)$$

We used the gamma matrices in the chiral representation (but of course the lagrangians (4) have the same form in any representation), and set the definitions:

$$\begin{cases} V_S = \frac{V_L + V_R}{2} \\ V_D = \frac{V_L - V_R}{2}. \end{cases} \quad (5)$$

The solutions of the equations of motion are easily obtained. In the Majorana case we search for the positive energy solutions of the form:

$$\nu^M(x) = \exp[-iE(\lambda)t + i\vec{p} \cdot \vec{x}] \times u(\lambda, \vec{p}); \quad (6)$$

where  $\lambda = \pm 1$  denotes the helicity:  $\vec{\Sigma} \cdot \vec{p} / p [u(\lambda, \vec{p})] = \lambda u(\lambda, \vec{p})$ , using the notation  $p$  for the squared three-momentum. Since the spinor  $u$  obeys:

$$[E(\lambda)\gamma^0 - m - \gamma^0 \gamma^5 (\lambda p - V_L)] u(\lambda, \vec{p}) = 0 \quad (7)$$

the potential can be taken into account replacing

$$p \rightarrow p - \lambda V_L \quad (8)$$

in the usual formulae for energy and for spinors. In particular, the dispersion relation, depicted in fig. 1, becomes:

$$E(\lambda) = \sqrt{m^2 + (\lambda p - V_L)^2}. \quad (9)$$

The steps (6-9) can be repeated for the Dirac field, since after the simple replacement:

$$V_L \rightarrow V_D \quad (10)$$

the wave  $\nu^D(x) = \exp(iV_S t) \nu^D(x)$  is shown to obey the same equation of  $\nu^M(x)$ .

The quantization of the Majorana field yields us:

$$\nu^M(x) = \sum_\lambda \int \frac{d\vec{p}}{2E(\lambda)(2\pi)^3} \left[ a(\lambda, \vec{p}) u(\lambda, \vec{p}) e^{-iE(\lambda)t + i\vec{p} \cdot \vec{x}} + \xi a^\dagger(\lambda, \vec{p}) \overline{C u(\lambda, \vec{p})}^t e^{+iE(\lambda)t - i\vec{p} \cdot \vec{x}} \right], \quad (11)$$

where spinors and operators are normalized to  $2E(\lambda)$ , and  $\xi$  is a phase factor entering the Majorana condition:  $C\overline{\nu^M(x)}^t = \xi\nu^M(x)$ . In order to obtain the quantized Dirac neutrino  $\nu^D$  one has (i) to replace the creation operator  $a^\dagger$  in (11) with a different degree of freedom  $b^\dagger$ , (ii) perform the substitution (10) into the expressions for energy and for spinors, and finally (iii) multiply the resulting field  $\nu'$  by the phase  $\exp(-iV_S t)$ . Due to this last step,  $V_S$  will enter in the expression for the energy of a Dirac neutrino (resp. antineutrino) as:  $E(\lambda) + V_S$  (resp.  $E(\lambda) - V_S$ ).

## 2 $\beta$ -spectrum

The  $\beta$ -decay is due to the charged current lagrangian:

$$\mathcal{L}_{CC} = -\frac{G_F \cos \theta_C}{\sqrt{2}} \bar{u}\gamma^a(1 - \gamma^5)d \bar{e}\gamma_a(1 - \gamma^5)\nu, \quad (12)$$

where  $\nu = \nu^M$  or  $\nu^D$ . The potentials modify the  $\beta$ -spectrum. In this section we describe in detail the modifications which take place for a Majorana neutrino, and indicate how to adapt the formulae to the Dirac case. To be concrete, we will focus on the tritium decay:

$${}^3\text{H} \rightarrow {}^3\text{He} + e + \bar{\nu}, \quad Q = 18590 \text{ eV (ref. [6])} \quad (13)$$

for which the energy release  $Q$  (the nuclear mass difference being  $\Delta M = m_e + Q$ ) is so small that all particles except possibly the antineutrino can be considered non-relativistic.

The matrix element squared is:

$$|\mathcal{M}(\lambda)|^2 = \text{const.} \times (E_\nu(\lambda) + \lambda p_\nu - V_L), \quad (14)$$

where the constant depends on the fundamental parameters in (12), on the nuclear matrix element and on the masses of the electron and of the nuclei (one simple derivation of this result: consider the usual result for  $|\mathcal{M}|^2$  for neutron decay, substitute  $(p_\nu)^a$  with  $(p_\nu)^a + \lambda m_\nu (n_\nu)^a$  to account for antineutrino polarization, perform the replacement (8) and then take the non-relativistic limit). For the Dirac case, use (10). As expected, the matrix element corresponding to the positive helicity dominates in the relativistic limit.

Since the antineutrino energy depends on the polarization, the maximal electron energy will also depend on it. The minimal antineutrino energy is  $E_\nu^{\min} = m_\nu$  if  $\lambda = \text{sign}(V_L)$ , or  $E_\nu^{\min} = \sqrt{m_\nu^2 + V_L^2}$  if  $\lambda = -\text{sign}(V_L)$ . Therefore, from the energy conservation condition we obtain:

$$E_e^{\max}(\lambda) = \begin{cases} \Delta M - m_\nu & \text{if } \lambda = \text{sign}(V_L) \\ \Delta M - \sqrt{m_\nu^2 + V_L^2} & \text{if } \lambda = -\text{sign}(V_L). \end{cases} \quad (15)$$

The first case corresponds to a non-zero minimum momentum of the antineutrino:  $p_\nu = |V_L|$ . For the Dirac neutrino, in order to obtain the maximum electron energy one has (i) to perform the replacement (10) and (ii) to add  $V_S$  in the previous formula.

Let us consider the phase space of the reaction. Using the delta function from momentum conservation to integrate away the helium-3 three-momentum, integrating over the possible direction of the electron, and averaging over those of the antineutrino we get:

$$d\Phi_3(\lambda) = \frac{1}{(2\pi)^3} \frac{p_e^2 dp_e}{2E_e E_{3\text{He}}} F_\nu(\lambda), \quad F_\nu(\lambda) = \frac{p_\nu^2 dp_\nu}{E_\nu(\lambda)} \delta(\Delta M - E_e - E_\nu(\lambda)) \quad (16)$$

where  $F_\nu(\lambda)$  is a phase space factor related to the antineutrino degrees of freedom. When integrating over the unobservable antineutrino momentum, one has to take into account the dependence of the energy on the helicity:

(1) If  $E_e < \Delta M - \sqrt{m_\nu^2 + V_L^2}$  (corresponding to  $E_\nu > \sqrt{m_\nu^2 + V_L^2}$ , see fig. 1), there are two possible momenta, one for each helicity state:  $p_\nu = \sqrt{E_\nu^2 - m_\nu^2} + \lambda V_L$ . For them we get:

$$F_\nu(\lambda) = \frac{(\sqrt{E_\nu^2 - m_\nu^2} + \lambda V_L)^2}{\sqrt{E_\nu^2 - m_\nu^2}} \Big|_{E_\nu = \Delta M - E_e} \quad (17)$$

(2) In the case  $E_e > \Delta M - \sqrt{m_\nu^2 + V_L^2}$  there is only one helicity state,  $\lambda = \text{sign}(V_L)$ , but there is a second value of the momentum at fixed energy:  $p_\nu = -\sqrt{E_\nu^2 - m_\nu^2} + \lambda V_L$ . The phase space factor for this determination of the momentum is:

$$F_\nu(\lambda) = \frac{(\sqrt{E_\nu^2 - m_\nu^2} - \lambda V_L)^2}{\sqrt{E_\nu^2 - m_\nu^2}} \Big|_{E_\nu = \Delta M - E_e} \quad (18)$$

whereas, for the other momentum, formula (17) applies (with the same value of the helicity). Notice that this phase space factor is formally identical to the one that we would obtain using the  $\lambda = -\text{sign}(V_L)$  and  $p_\nu = \sqrt{E_\nu^2 - m_\nu^2} + \lambda V_L$ , even if, strictly speaking, this ‘‘square momentum’’  $p_\nu$  is negative.

The differential spectrum of the electron can be estimated by summing up the antineutrino helicities,  $d\Gamma = \sum_\lambda d\Phi_3(\lambda) |\mathcal{M}(\lambda)|^2 / (2 m_{3\text{He}})$ , where as discussed above, both the matrix elements (14) and the phase space (16) depend on the helicity:

$$\frac{d\Gamma}{dE_e} \propto p_e E_e F(Z, E_e) \times \sum_{\sigma=\pm 1} \frac{E_\nu + \sigma \mathcal{P}_\nu}{2 \mathcal{P}_\nu} (\mathcal{P}_\nu + \sigma V_L)^2 \Big|_{E_\nu = \Delta M - E_e} \quad (19)$$

in this formula  $p_e = \sqrt{E_e^2 - m_e^2}$  and  $\mathcal{P}_\nu = \sqrt{E_\nu^2 - m_\nu^2}$ ;  $F(Z, E_e)$  embodies the electromagnetic corrections due to the interaction of the final states. The maximal electron energy is

$$E_e^{\text{endp.}} = \Delta M - m_\nu \quad [\text{Majorana}], \quad (20)$$

and is not shifted by the potential  $V_L$  (we recall that  $\Delta M$  denotes the  ${}^3\text{H}-{}^3\text{He}$  mass difference).

In the Dirac case we get:

$$\frac{d\Gamma}{dE_e} \propto p_e E_e F(Z, E_e) \times \sum_{\sigma=\pm 1} \frac{E_\nu + \sigma \mathcal{P}_\nu}{2 \mathcal{P}_\nu} (\mathcal{P}_\nu + \sigma V_D)^2 \Big|_{E_\nu=\Delta M - E_e - V_S}. \quad (21)$$

The maximal electron energy is

$$E_e^{\text{endp.}} = \Delta M - m_\nu + V_S \quad [\text{Dirac}], \quad (22)$$

and therefore differs from the Majorana case if  $V_S \neq 0$ .

The Kurie plot is defined as:

$$K(E_e) = \sqrt{\frac{1}{p_e E_e F} \frac{d\Gamma}{dE_e}}; \quad (23)$$

if masses and potentials are absent,  $K(E)$  turns out to be a line approaching zero at the endpoint. In the case of small neutrino mass the potential enters the formula for the Kurie plot as:

$$K(E_e) \propto |\Delta M - E_e + V_L|, \quad \text{small } m_\nu \quad (24)$$

for both Majorana and Dirac cases, but the endpoint is in a different position unless  $V_S = 0$  (compare eqs. (20) and (22)).

The integral spectrum, often used in the experimental analysis is:

$$I(E_e) = \int_{E_e}^{E_e^{\text{endp.}}} \frac{d\Gamma}{dE_e} dE_e. \quad (25)$$

### 3 Discussion of the results

We first discuss some typical features of the  $\beta$ -spectrum, and then compare them with the experimental results and with other theoretical models.

#### 3.1 Features of the $\beta$ -spectrum

We start with some general remarks on the differential spectrum, eqs. (19) and (21):

1. While the effects of the masses on the spectrum are of order  $(m_\nu/E_\nu)^2$ , the effects of the potential are of order  $V/E_\nu$ .
2. The Majorana and the Dirac neutrino spectra for equal masses are identical, not only if the potentials are absent, but under the weaker assumption  $V_S = 0$  (which, by definition (5), is equivalent to  $V_D = V_L$ ).

3. There is a curious behaviour of the differential spectrum at the endpoint: If the mass and the potential are both non-zero, it goes to infinity, since  $\mathcal{P}_\nu \rightarrow 0$  in eqs. (19) and (21). This fact however does not imply contradictions with the physical interpretation, since in any given finite interval the probability of transition is finite. This behaviour is due to the increasing number of states corresponding to a fixed energy interval when the neutrino energy decreases toward its minimum, compare with eqs. (16-18), or see fig. 1 (we recall that the minimum corresponds to the infinite-set of states  $\vec{p}_\nu = |V_L| \vec{n}_\nu$ , where the orientation  $\vec{n}_\nu$  is arbitrary)<sup>‡</sup>.

Continuing the discussion of the differential spectrum, we come to the differences between the Majorana and the Dirac cases. For a Majorana neutrino it is sufficient to distinguish if  $V_L$  is larger or smaller than zero. For small mass, in the first case the spectrum just translates upward, whereas in the second case it translates downward for energies  $E_e < \Delta M + V_L$ , where it becomes zero, and then it increases up to the endpoint (20): a dip is present. These features are clearly illustrated by eq. (24). The Dirac case is identical, apart for the fact that the position of the endpoint depends on  $V_R$ . Notice in particular that for  $V_L = V_R (= V_S, V_D = 0$  due to eq. (5)) the Kurie plot is simply a straight line which approaches zero at  $E_e = \Delta M + V_L$ .

Let us conclude with some comments on the integral spectrum. In the Majorana case, the integral spectrum for  $V_L > 0$  moves to the left, and approaches in a steeper fashion the endpoint when the mass is increased. Instead if  $V_L < 0$ , for masses of the order of  $|V_L|$  or smaller the integrated spectrum remains approximatively constant in the region that extends  $2|V_L|$  below the endpoint (the size of the dip in the differential spectrum). In the Dirac case for positive and increasing values of  $V_R$  the endpoint moves to the right, extending the region in which the integral spectrum stays approximatively constant, in accord with the features already discussed.

## 3.2 Comparison with the experimental results

Experimentally one can study the shape of the  $\beta$ -spectrum in the region far from the endpoint, or near the endpoint. Let us discuss these two regions in turn.

### 3.2.1 Region far from the endpoint

Due to the first feature of the spectrum emphasized in the previous subsection, a mass of some eV would give a deviation of the spectrum only near the endpoint, whereas a potential  $V_L$  of few eV would give a detectable shift of the spectrum also in the region far from the endpoint (the eV range being the present experimental accuracy). In this

---

<sup>‡</sup>If the potential  $V_L$  is zero, the minimum shifts at  $p_\nu = 0$ , and therefore the phase space factor  $d\vec{p}_\nu$  shrinks to zero when the minimum is approached, whereas if  $m_\nu = 0$  the dispersion relation curve in this limit does not flatten, so that the phase space attains a finite value.

hypothesis, the experiments which measure the  ${}^3\text{H}-{}^3\text{He}$  mass difference fitting the  $\beta$ -spectrum far from the endpoint are sensitive to  $\Delta M|_{\beta} = \Delta M + V_L$  (eq. (24) applies since the neutrino energy is much larger than its mass in the region under discussion) which would systematically deviate from the  $\Delta M|_{\text{non-}\beta}$ , obtained by techniques of measurement of the mass difference which do not rely on the  $\beta$ -spectrum. Whereas older data were to some extent indicative of a discrepancy between the  $\beta$ - and the non- $\beta$ -determinations of  $\Delta M$ , more recent and precise determinations are in remarkable agreement [7]. Including the six more recent measurements reported in ref. [7] (5  $\beta$ - and 1 non- $\beta$ -techniques) we estimate:

$$V_L = \Delta M|_{\beta} - \Delta M|_{\text{non-}\beta} = 0.3 \pm 2.7 \text{ eV} \quad (26)$$

Eq. (26) rules out  $V_L > 5.6 \text{ eV}$  or  $V_L < -5.0 \text{ eV}$  at 95% CL.

### 3.2.2 Endpoint region

The region near the endpoint is very interesting for the search of electron antineutrino mass. Fits to recent data [3, 4] suggest a “negative masses squared”,  $m_{\nu}^2 \approx -20 \text{ eV}^2$ . Recalling the well-known feature that a (positive) neutrino mass term depletes the endpoint region of the differential spectrum, one realizes that a “negative mass squared” simply amounts to the fact that the measured spectrum is even larger than what one would expect postulating a massless neutrino. Putting aside the possibility of statistical or instrumental effects, such findings could be taken as suggestions of a peak-like structure near the endpoint region.

In the following we focus on the possibility to use the model under discussion to explain this feature. But before doing so, let us spend a few words of warning:

- Even if certain choices of the potentials are able to explain the presence of a peak in the endpoint spectrum, one should keep in mind that different types of patterns can be obtained with other choices of potentials (and, in particular, of their signs). In addition, other models exist which may entail modifications of the endpoint spectrum (see also the discussion below).
- The fit value:  $m_{\nu}^2 \approx -20 \text{ eV}^2$  quoted above is dominated by the experimental findings of the Troitsk collaboration [3], which reports the smallest errors, 4.8 and 5.8  $\text{eV}^2$ . The confidence level of the average fit values of [3] and [4] is of 0.6% or 20%, if we sum quadratically or linearly the statistical and the systematic errors (when they are quoted separately). These considerations suggest that it will be quite important to follow future experimental developments.

As it is clear from eq. (24), a Majorana neutrino with a small mass and a *negative* potential  $V_L$  of few eV could explain the appearance of a peak in the differential spectrum exactly at the endpoint, and a dip  $|V_L|$  electronvolts below. But for a Majorana



neutrino the position of the dip is linked to a downward shift of the spectrum in the region far from the endpoint, and therefore the bound (26) applies.

This limitation does not hold necessarily for a Dirac neutrino. In fact, if  $V_L \sim 0$  and  $V_R$  is *positive*, there is no deviation in the differential spectrum up to the point in which it vanishes,  $E_e = \Delta M$ , but for larger energies the spectrum would start to rise constantly, up to the endpoint  $E_e = \Delta M + V_R/2$  (we assumed again a small neutrino mass term). We conclude that a potential  $V_R$  of some eV, felt by a Dirac neutrino, can manifest itself in a peak of the differential spectrum near the endpoint region. A  $V_R$  in the twenty eV range or so can already be excluded by the data. Let us stress that in such a scheme there is no need to attach any physical meaning to the “negative mass squared”.

### 3.3 Comparison with other theoretical models

An observable deviation of the spectrum in the region far from the endpoint region (eq. (26) and related discussion), characterizes the scenario in which the neutrino propagates in a (large) background potential  $V_L$ .

Instead, peak-like structures in the endpoint region can also arise in the presence of a degenerate neutrino sea, filled up to the Fermi level  $\mu_F$  [8]. In fact, the reaction of absorption of a neutrino  $\nu_{\text{sea}} + {}^3\text{H} \rightarrow e + {}^3\text{He}$  permits the emission of electrons with energies between  $\Delta M$  and  $\Delta M + \mu_F$ , if the neutrino mass is supposed to be small in comparison with  $\mu_F$ . Therefore, one cannot discriminate between these two theoretical possibilities from the experimental information on the  $\beta$ -spectrum. Instead, if neutrino masses are not small it is possible, at least in principle, to distinguish between the two cases (*i.e.* potential *versus* chemical potential). In fact, if we suppose the existence of a degenerate sea of massive neutrinos, no electron could be emitted in the energy range between  $\Delta M - m_\nu$  and  $\Delta M + m_\nu$  (the emission due to the neutrino absorption taking place for larger energies, up to  $E_e = \Delta M + m_\nu + \mu_F$ ) [9]. Such a discontinuity of the differential spectrum is absent in the models discussed in the present work.

## Acknowledgments

I wish to thank A.Yu. Smirnov who suggested the question studied in the present work, and to acknowledge discussions with S. Cherubini, S. Esposito and S. Pakvasa.

## References

- [1] L. Wolfenstein, Phys.Rev. D17 (1978) 2369.
- [2] J.I. Collar, preprint hep-ph/9611420.
- [3] A.I. Belesev *et al.*, presented at the XVII Conference on Neutrino Physics and Astrophysics, Helsinki, 13-19 June 1996;  
A.I. Belesev *et al.*, Phys.Lett. B 350 (1995) 263.
- [4] H. Backe *et al.*, presented at the XVII Conference on Neutrino Physics and Astrophysics, Helsinki, 13-19 June 1996;  
W. Stoeffl and D. Decman, Phys.Rev.Lett. 75 (1995) 3237;  
Ch. Weinheimer *et al.*, Phys.Lett. B 300 (1993) 210;  
E. Holzschub *et al.*, Phys.Lett. B 287 (1992) 381;  
H. Kawakami *et al.*, Phys.Lett. B 256 (1991) 105;  
R.G.H. Robertson *et al.*, Phys.Rev.Lett. 67 (1991) 957.
- [5] J. Pantaleone, Phys.Lett. B 268 (1991) 227.
- [6] R.S. Van Dyck *et al.*, Phys.Rev.Lett. 70 (1993) 2888.
- [7] See for example table II of the previous reference, in which the historical excursus of the determinations of  $\Delta M$ , and the references to the previous works are presented.
- [8] S. Weinberg, Phys.Rev. 128 (1962) 1457.
- [9] J.M. Irvine and R. Humphreys, J.Phys. G9 (1983) 847.

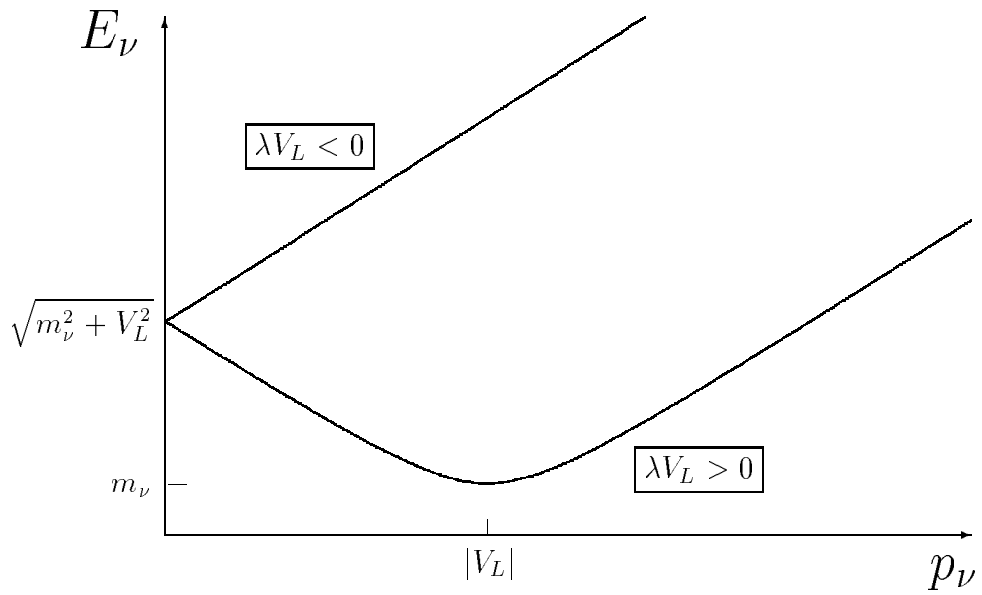


Figure 1: Dispersion relation for Majorana neutrinos in presence of a constant potential  $V_L$ .